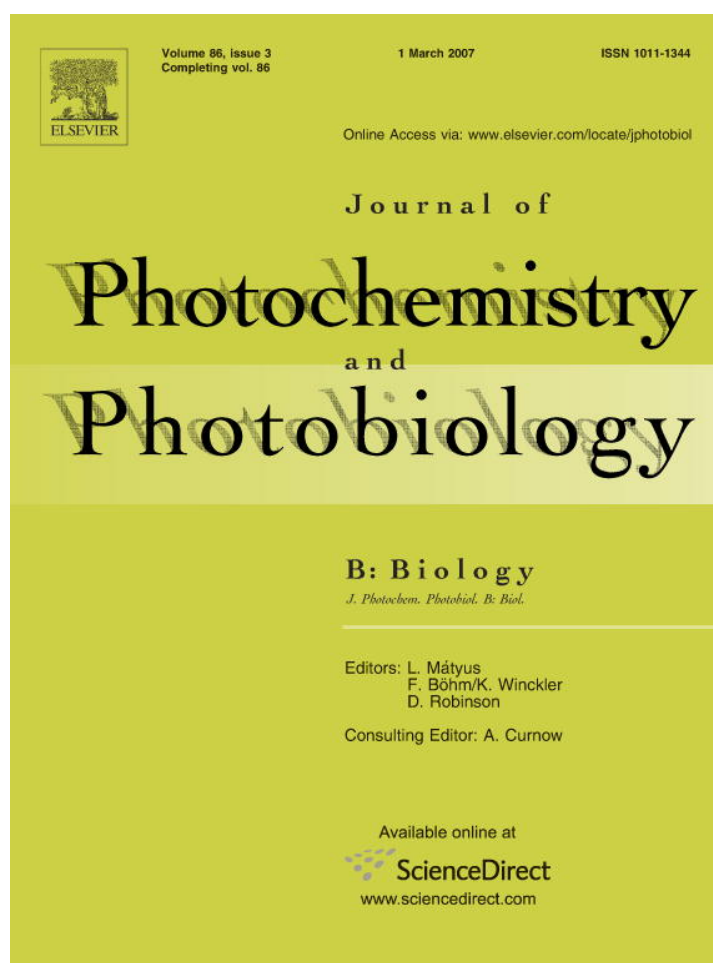


Provided for non-commercial research and educational use only.
Not for reproduction or distribution or commercial use.



This article was originally published in a journal published by Elsevier, and the attached copy is provided by Elsevier for the author's benefit and for the benefit of the author's institution, for non-commercial research and educational use including without limitation use in instruction at your institution, sending it to specific colleagues that you know, and providing a copy to your institution's administrator.

All other uses, reproduction and distribution, including without limitation commercial reprints, selling or licensing copies or access, or posting on open internet sites, your personal or institution's website or repository, are prohibited. For exceptions, permission may be sought for such use through Elsevier's permissions site at:

<http://www.elsevier.com/locate/permissionusematerial>



Effect of low intensity laser interaction with human skin fibroblast cells using fiber-optic nano-probes

Gopalendu Pal^a, Ashim Dutta^a, Kunal Mitra^{a,*}, Michael S. Grace^b, Albert Amat^d, Tara B. Romanczyk^c, Xingjia Wu^c, Kristi Chakrabarti^{c,d}, Juanita Anders^c, Erik Gorman^d, Ronald W. Waynant^d, Darrell B. Tata^d

^a Department of Mechanical and Aerospace Engineering, Florida Institute of Technology, 150 W University Blvd, Melbourne, FL 32901, United States

^b Department of Biological Sciences, Florida Institute of Technology, Melbourne, FL 32901, United States

^c Uniformed Services University of the Health Sciences, Bethesda, MD 20814, United States

^d Food and Drug Administration, Rockville, MD 20857, United States

Received 30 August 2006; received in revised form 1 December 2006; accepted 1 December 2006

Available online 16 January 2007

Abstract

Over the past forty years, many efforts have been devoted to study low power laser light interactions with biological systems. Some of the investigations were performed in-vitro, on bulk cell populations. Our present work was undertaken to apply specially engineered fiber-optic based nano-probes for the precise delivery of laser light on to a single cell and to observe production of low power laser light induced reactive oxygen species (ROS). A normal human skin fibroblast (NHF) cell line was utilized in this investigation and the cells were irradiated under two different schemes of exposure: (1) an entire NHF cell population within a Petri dish using a fan beam methodology, and (2) through the precise delivery of laser energy on to a single NHF cell using fiber-optic nano-probe. Photobiostimulative studies were conducted through variation of laser intensity, exposure time, and the energy dose of exposure. Laser irradiation induced enhancement in the rate of cell proliferation was observed to be dependent on laser exposure parameters and the method of laser delivery. The total energy dose (fluence) had a greater influence on the enhancement in the rate of cellular proliferation than compared to laser intensity. The enhancement in the growth rate was observed to have a finite life-time of several days after the initial laser exposure. Fluorescent life-time imaging of ROS was performed during the nano-based single cell exposure method. The kinetics of ROS generation was found to depend strongly on the laser fluence and not on the laser intensity.

© 2006 Elsevier B.V. All rights reserved.

Keywords: Cell proliferation; Fluorescence life-time imaging; Low level light therapy (LLLT); Low power laser irradiation; Nano-probes; Reactive oxygen species

1. Introduction

Low level laser therapy (LLLT) involves interaction of a low power monochromatic light with biological systems in order to initiate biomodulative effects. Photon induced biomodulation (i.e., photobiomodulation) was the subject of several studies over the past few years. Low level laser exposures have produced both stimulative and inhibitory

effects in-vitro and in-vivo, depending on the energy dose (i.e., fluence). Traditionally, red to near IR wavelength light have been used for LLLT due to superior penetration depth into tissue. A majority of the low level laser induced photobiomodulative studies were performed with the He–Ne lasers [1–3]. For in-vivo applications, beneficial effects of LLLT were found in wound healing [4], peripheral and central nerve regeneration [5], and for the treatment of stomach and duodenal ulcers [1]. However, not all observations to date have reported on positive effect of LLLT. A study by Broadley et al. reported no beneficial

* Corresponding author. Tel.: +1 321 674 7131; fax: +1 321 674 8813.
E-mail address: kmitra@fit.edu (K. Mitra).

effect of LLLT on tensile strength of incisional wounds [6]. Similarly, Allendorf et al. and Lowe et al. demonstrated no beneficial effect of laser irradiation on wound healing in rats [7–9].

For in-vitro studies at the cellular level, LLLT was found to alter gene expression [4], cellular proliferation [1,2,10,11], inter-cellular pH balance [12], mitochondrial membrane potential [12], generation of transient reactive oxygen species [12–15] and calcium ion level [12,16,17], proton gradient [18] and consumption of oxygen [19]. An increase in the proliferation of fibroblasts, keratinocytes, myeloma, myotube, squamous carcinoma and urothelial (both normal and carcinoma) has already been reported in the literature for extremely low doses of laser irradiation [1,20,21]. On the other hand, an inhibitory effect was observed at higher energy doses [10]. Irradiation of light at wavelengths of 630 nm, 632.8 nm and 820 nm were found to accelerate ATP synthesis in R3230 AC mammary adenocarcinoma cells [22], human peripheral lymphocyte cells [23], and He–La cells [1].

Monitoring the biochemical changes taking place during and immediately after LLLT is of importance in order to understand the underlying processes and mechanisms of interaction between low intensity light and the biological system to achieve biomodulative effects. Several theories have been put forward to explain the transient and permanent biochemical changes due to LLLT. Data on stimulative and inhibitive action of blue and red light on mammalian and bacterial cells were reviewed [1,24]. Karu proposed that effects on cytochrome oxidase associated with the respiratory chain of mitochondria to be a plausible mechanism. Mechanistically it was proposed that two processes are involved during the light-cell interaction. One of them is the acceleration of the electron transfer in the redox pairs in some sections of the respiratory chain, and the other, the transfer of the excitation energy to molecular oxygen resulting in a formation of reactive oxygen species (ROS). The former process is suspected to dominate at lower energy doses producing biostimulation, whereas, photodynamic damage occurs at the higher energy dose [1]. Lubart et al. [25], found incident broad band irradiation between wavelength range of 400–800 nm to increase of calcium ion (Ca^{2+}) within the cytoplasm of cardiomyocytes. A correlation in cardiomyocytes was observed: at a lower laser energy doses of exposure, a small and transient rise in the intracellular Ca^{2+} levels were observed, whereas at higher fluence, intracellular Ca^{2+} levels were substantially increased for considerably longer durations.

Thus, as per the mechanisms proposed during LLLT, detection of Ca^{2+} and ROS is of importance for understanding the transient biochemical phenomena for LLLT. Detection of both Ca^{2+} and ROS is necessary for comparative study to understand which biochemical phenomenon is occurring first and through which possible route. Among the studies related to Ca^{2+} detection, intracellular Ca^{2+} movement was also reported to play a pivotal role in the

control of sperm motility [26]. It was shown that Ca^{2+} transport in sperm cells was affected by factors acting in the mitochondria [27]. LLLT at 632.8 nm was also reported to increase Ca^{2+} level in human lymphocytes and rat neurons in-vitro with the existence of an optimal energy density to achieve biomodulative effects [16].

In the last two decades, an important area of investigation was the identification of short lived, highly reactive oxygen species in biological systems. As mammalian cells exist in a constant oxidative siege requiring an appropriate balance of oxidants and anti-oxidants, inducement of either was found to modulate biological processes [28,29]. There was increasing evidence to suggest that very low and controlled concentrations of ROS participate in signal transduction mechanisms [30]. In the case of spermatozoa, ROS such as super oxide anion, hydrogen peroxide and nitric oxide were found to induce sperm hyperactivation, capacitation or acrosome reaction [31]. Generation of ROS in live cells during LLLT was studied by Callaghan et al. [32] and Lubart et al. [13]. The focus of this paper is to deliver low power laser precisely to a single cell using nano-probes and monitor the generation of ROS during LLLT by time-resolved fluorescence life-time imaging.

Recent advances in nano-technology leading to the development of optical fibers with sub-micron sized dimensions have opened up new horizons for intercellular measurements. Fiber-optic based chemical sensors [33,34], biosensors [35] were found to offer important advantages for in situ monitoring applications [36]. This ability provides a great deal of promise for selective sensing of species in small environments where spatial resolution is critical. Recently, fiber-optic nano-biosensors were developed for intracellular measurement of pH, calcium, oxygen, and absorption of glucose molecules by living cells [37–39]. The use of sub-micron tapered optical fibers was also demonstrated and used to investigate the possible spatial resolution obtained using near field microscopy [40]. One of the advantages of these nano-sensors is in the probing of individual cells to obtain biochemical information. These nano-sensors offer a number of unique properties such as low attenuation losses, microscale transverse dimensions, long interaction length, flexibility, electrically passive operation, delivery of non-ionizing radiation, high sensitivity and could be modified for multi-parameter measurements. Such advanced features have made nano-optical fibers an ideal medium for laser delivery and sensing that recently showed a significant impact on various modern bio-photonics systems.

In the past, investigations have primarily been performed on populations of cells. Little is known about the effects of low power laser irradiation on a single cell or within subcellular organelles. Effects of laser irradiation on single cells have been studied by Alexandratou et al. [12,41] and Powell [42] using confocal microscopy and fluorescence imaging technique. In their investigations, a single cell was precisely irradiated by He–Ne laser and fluorescence life-time imaging of ROS, Ca^{2+} , intra-cellular pH,

and cell viability was performed using confocal microscopy. The effects of low power laser-cell interaction were investigated only for a single laser energy dose in these past studies. The bio-effect of various energy doses, laser intensities, exposure times, and fiber guided precise laser delivery to a single cell were not considered. The changes in the redox state of the respiratory chain during low power laser irradiation of a single cell were investigated by Lapotko et al. [43] using photothermal (PT) microscopy technique. The cells were found to respond to the low power laser by changing their redox state [43].

In this communication, the use of specifically engineered fiber-optic based nano-sensor probes for the precise delivery of light to a targeted normal human skin fibroblast (NHF) cell is reported. The cells were irradiated under two exposure schemes. Firstly, experiments were performed by irradiating the whole cell population for the purpose of comparison with a single cell irradiation. Secondly, low power laser light was delivered precisely to an individual cell using fiber-optic nano-probes. For both cases, cell proliferation rates were monitored. Finally experiments were conducted to capture time-dependent fluorescence signals emitted due to generation of ROS from a single cell when precisely irradiated with laser using a nano-probe. Studies were performed with variation of laser intensity, exposure time, and total energy doses for all of the above cases.

2. Materials and methods

2.1. Fabrication of nano-fibers

Since optical fibers with submicron size diameter cores are not commercially available, an important aspect of this work involved fabrication of reproducible nano-probes for in-vivo studies. Nano-fibers were fabricated by pulling larger silica optical fibers (core diameter 125 μm) with the aid of a micropipette stretching device that had been optimized for pulling silica fibers. During pulling of optical fibers appropriate heating was applied either by a thinly-stream torch or with a CO_2 laser. Using this pulling device method, fibers with submicron size diameter (typically 20 nm) of one end were produced. Similar fiber-optic tips could also be fabricated by etching with suitable chemical solutions.

Due to the small diameter of this fiber tip, light used to excite the sample cells, was trapped inside the fiber, and a near field excitation process occurred. The small near field spot-size in turn yielded the excitation volume of the sample down to the cubic nanometer scale. However, by tapering these fibers to such small diameters in a pulling process, (such as micropipette puller technique described above) the cladding around the core of the optical fiber was stretched remarkably thin that total internal reflection no longer occurred within the fiber. The resulting loss of the excitation light caused a severe reduction in the intensity of the evanescent field at the tip of the fiber. To prevent energy

leakage, the outside wall of the fiber near the tapered end was coated with silver down to approximately a few hundred nanometers of thickness. The silver coating process was done in a thermal evaporator system. As the vacuum deposition process began, the fibers, which were mounted on a rotating stage, were spun to ensure that an even coating of silver was applied to all sides. The tips of the fiber were shadowed from the silver, leaving a free silica surface on the distal end of the fiber. Typical fiber tip diameters of metal-covered bio-probes were in the order of 200–500 nm as measured under the light microscope and shown in Fig. 1.

2.2. Cell culture

Normal human skin fibroblast (NHF) cell lines were purchased from ATCC (American Type Culture Collection, ATCC # CRL-2522) and used throughout this study. The cells were grown in Eagle's minimum essential medium (MEM) with L-glutamine, and sodium citrate, supplemented with 1–2% (v/v) penicillin G sodium and streptomycin sulfate (Invitrogen), and 10% (v/v) fetal bovine calf serum (Sigma–Aldrich). Cultures were maintained at a constant temperature of 37 $^{\circ}\text{C}$ in an atmosphere of 95% air and 5% CO_2 . Live NHF cells adhered to the bottom of the petri dish with typical fibroblast morphology whereas dead cells floated freely in the culture medium and were removed either during medium renewal or rinsing prior to trypsinization for cell counting. A solution of 0.25% trypsin and 0.53 mM EDTA (purchased from ATCC) was used suspend cells for counting or when passaging cells to new dishes. Non-irradiated cultures were passaged at a dilution of 1:4 every two days. Cell counting was performed using a hemacytometer in regular intervals of every two days. In a few cases, cells were also counted using a Coulter counter for corroboration of the hemacytometer counts.

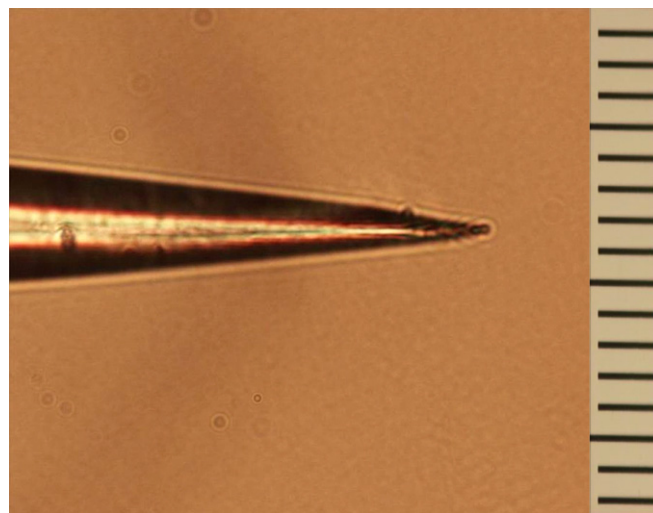


Fig. 1. Image of the tip of a nano-probe (vertical scale 10 $\mu\text{m}/\text{div}$).

2.3. Fluorescence imaging chemicals

Dichlorodihydrofluorescein diacetate (H_2DCFDA ; Molecular Probes Inc.) was used as fluorescent labeling dye to probe the generation of ROS. H_2DCFDA detects ROS such as hydrogen peroxide, singlet oxygen and hydroxyl radicals in living cells, but not superoxide anions or nitric oxides. When activated by ROS, H_2DCFDA has excitation and emission maxima wavelengths of 492–495 nm and 517–527 nm, respectively. For experimental analyses, growth medium was removed and cultures were washed with phosphate buffered saline (PBS). Cells were loaded with 6 μM H_2DCFDA in PBS and incubated for 30 min. After incubation, cultures were placed into pre-warmed complete growth medium and incubated for 10 min to allow cleavage of the AM-ester groups of H_2DCFDA . Finally the cells were washed again in PBS to remove dye present in growth medium prior to fluorescence imaging.

2.4. Laser stimulation

2.4.1. Entire cell population exposure

NHF cells in suspension were exposed to low levels of diverging fan beam He–Ne laser light on day 0. Total energy dose (Joules/cm²) and laser intensity (mW/cm²) of exposure were varied within a range of 0.5–16 J/cm² and 0.64–1.16 mW/cm², respectively. The irradiated and (sham exposed) control cells were placed inside the incubator after the treatment. Cell counting was performed in regular intervals of 2 days for both irradiated and control cells. The cells were allowed to proliferate in the same Petri dish to investigate the absolute proliferation rates under same culture condition.

2.4.2. Single cell exposure

Experiments were conducted by delivering laser radiation to individual cells through fabricated nano-probes. The beam emitted from the nano-probe was measured by light microscopy to have a spot diameter of 200 μm .

Single cells were irradiated within the same energy fluence range as the entire population treatment conditions of 0.5–16 J/cm² at several laser intensities ranging from 330 mW/cm² to 20 W/cm². All irradiated conditions had their sham exposed control counterparts in which their surrounding environment was identical to the laser treated condition. To investigate the single cell growth characteristics for the case of a single cell exposure, the laser exposed single cell was observed under high resolution phase contrast microscopy in regular interval of 2 days, in order to qualitatively estimate the cellular proliferation rather than counting the bulk cell population using hemacytometer. The irradiated area in the petri dish was marked to ensure the monitoring of proliferation of the same irradiated cell. The laser induced ROS generation of a single cell was monitored quantitatively by fluorescence life-time imaging which involved capturing temporally decaying signals from single cell using a fluorescence imaging microscope.

2.5. Experimental set-up

2.5.1. Single cell exposure

The schematic representation of the experimental set-up is shown in Fig. 2. A continuous wave He–Ne laser (Newport Corporation) of 632.8 nm wavelength was used as the LLLT source. The laser beam was fed into the larger end of the nano-fiber via a converging lens and a collimator. The low power laser beam was delivered to the desired location of an individual cell using nano-size tip of the same fiberoptic probe. The movements of the nano-probes were operated using 3-axis micromanipulators. The exact location of the nano-probes tip within the cell culture was precisely determined by an inverted microscope. The cells were placed in Petri dishes and positioned on the stage above the objective lens. The cells in the Petri dish were trypsinized and fully dispersed in the culture medium and then targeted by a nano-probe.

Fluorescence life-time imaging of ROS from a single cell was performed after precisely irradiating a single cell with the nano-probe using a 632.8 nm wavelength He–Ne laser beam. An excitation light source of wavelength 488 nm was used to illuminate the laser irradiated cell for fluorescence life-time imaging. The fluorescence emitted from the sample due to generation of ROS was detected at wavelength of 522 nm. The emitted fluorescent signals from the cell were collected by another optical fiber and fed to the CCD camera (Model DVC-4000, DVC Company) which was in turn connected to the computerized data acquisition system. The band pass filter set (purchased from Chroma Technology Corporation) used for this study had excitation and emission bands at 480–495 nm and 517–527 nm, respectively. Fluorescent images were captured in the regular intervals using Image-Pro Plus V4.1 software and the captured images were processed using National Instruments image processing software IMAQ Vision Builder 6.0 and yielded temporal fluorescent intensity spectra.

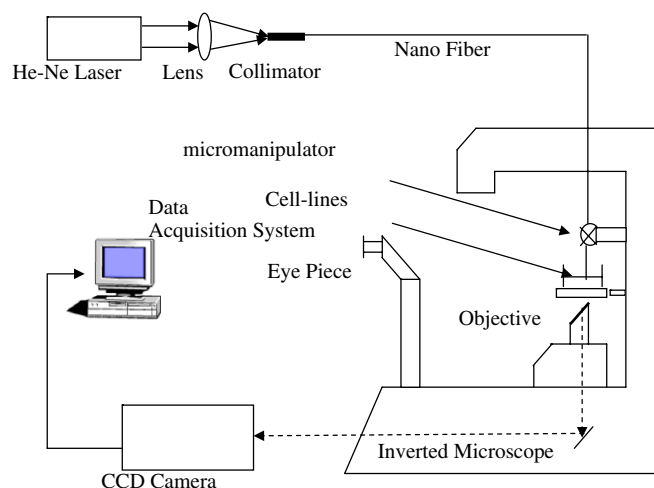


Fig. 2. Schematic of experimental set-up.

2.5.2. Entire cell population exposure

Laser exposures of entire cell population were performed in Petri dish and a fan beam was used to illuminate the Petri dish. The laser beam emitted from the source was allowed to pass through a diverging lens forming a fan beam which had a diameter of 35 mm (same as the diameter of the Petri dish in which the cells were in culture). The cells were counted using a hemacytometer and Coulter counter.

2.6. Statistical analyses

During the analysis of cell proliferation in different control sets the variation of cell proliferation among control sets were statistically assayed using ANOVA. However, when analyzing responses of cell cultures to laser irradiation, variances among replicates were found to be inhomogeneous. Therefore, statistical comparisons between mean values of laser-irradiated cells and control cells were performed using Welch's *t*-test, and $p < 0.05$ was considered significant. Standard error of the mean for experimental data was calculated and they are represented in the form of error bars in figures wherever applicable.

3. Results and discussion

Interactions of low power laser light with cells have been proposed to yield bio-stimulative effects. In part, these LLLT effects are manifested in terms of modulation in the rate of cellular proliferation and transient biochemical changes. In this work, cell proliferation was investigated under the exposure scheme where the entire cell population was irradiated using a diverging fan beam. Variation of laser intensity and energy dose were performed to investigate the stimulative effects of laser irradiation.

To gain insight in the stimulative effect of low power laser on cells, we studied time-dependent processes taking place after laser irradiation. In this investigation, the generation of ROS was monitored after precisely irradiating a single cell using a nano-probe through fluorescence life-time imaging. The fluorescence life-time imaging of the H₂DCFDA probe gave the time scale and magnitude of ROS production due to laser irradiation.

3.1. Proliferation in control cell cultures

Before investigating the effect of laser irradiation on cell proliferation rate, it was necessary to determine the proliferation rate of sham exposed (control) cells. Cells without laser irradiation were counted at 2 day intervals. Cell proliferation rates of control cell cultures are shown in Fig. 3. Three sets of control cells were sham exposed and grown in identical culture conditions as the laser treated conditions. Equal numbers of cells were seeded in each of the culture dishes, and then at 2-day intervals, cells were trypsinized and suspended in equal volumes of growth medium. The number of cells per unit volume (ml) is plotted with respect

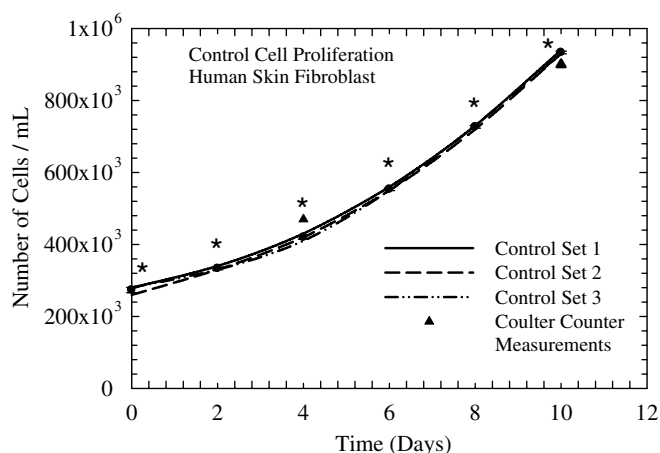


Fig. 3. Number of cells per unit volume for un-irradiated control cultures measured using a hemacytometer and by automated Coulter counter. * Deviation among cell counting for different cultures in the particular day is insignificant (ANOVA test, $p > 0.05$); error bars smaller than symbol size are omitted.

to time (days) in Fig. 3 for three such cases. The growth curves are essentially identical in each of the three sets of cultures (from day 2 to day 10, total cell counts differed among culture sets by only 1.1–3.0%, $p > 0.05$). On days 4 and 10, cells were also counted using a Coulter counter to corroborate hemacytometer counts. Cell counts obtained using Coulter counter coincide well with those obtained using the hemacytometer.

To characterize the rate of cell proliferation, a parameter termed “ratio of cell proliferation” is used. This is defined as the ratio of the number of cells per unit volume on a given day to the number of cells per unit volume on the immediately previous count day (2 days prior in each case). Thus, the higher the value of this ratio, the greater the rate of cell proliferation. In Fig. 4, the ratio of cell proliferation is plotted as a function of time (days) for the control cultures shown in Fig. 3. Cells in each of the three sets

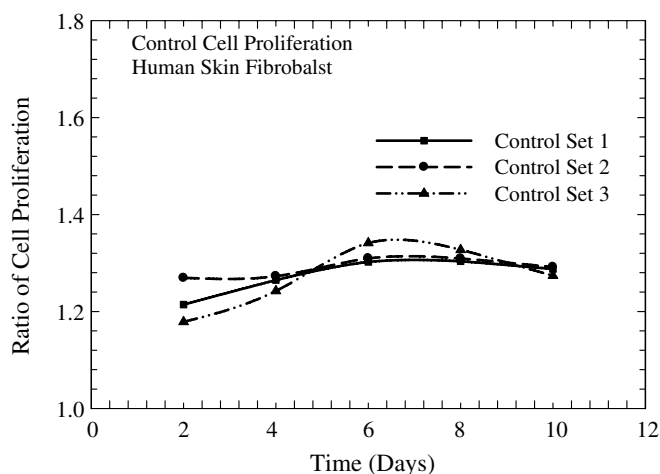


Fig. 4. Rate of cell proliferation in un-irradiated control cultures (ratio = number of cells on day indicated divided by that measured 2 days before).

grew at the same general rate (average rate of increase in cell number = 1.2 per 2-day interval).

3.2. Irradiation of cell populations

To investigate the effects of laser irradiation on cell proliferation, whole cultures were irradiated with a diffuse laser beam with variation of laser intensity (mW/cm^2) and energy dose (J/cm^2). The collimated laser beam from a He–Ne laser source was passed through a diverging lens to create a fan beam which had a radius of 35 mm when illuminating the entire surface area of the Petri dish. The cell proliferation dependence on the total energy dose was studied by keeping the laser intensity constant at $1.16 \text{ mW}/\text{cm}^2$ and irradiating the cell population for different time durations. Cultures increased in population density faster after laser stimulation than in controls with no laser stimulation (Fig. 5). The effect appeared to be dose-dependent; increasing energy dose caused faster increase in cell numbers over the range of doses tested ($8\text{--}16 \text{ J}/\text{cm}^2$). At the highest doses (10 and $16 \text{ J}/\text{cm}^2$), cell numbers began to reach a plateau by days 10–12 (Fig. 5). Therefore, analyses were performed on data from cell cultures up to 8 days post-stimulation.

The effects of laser energy dose on the rate of cell proliferation are shown in Fig. 6. Rate of cell proliferation was affected by laser irradiation in a dose-dependent manner. That is, cell proliferation rate was highest at an energy dose of $16 \text{ J}/\text{cm}^2$ and decreased with lower energy doses. Cell proliferation (and hence the rate of cell division) was greatest at the first observation time (2 days post-irradiation), and decreased over time (Fig. 6). At 2 and 4 days post-irradiation, proliferation was significantly greater at all irradiation doses than in control (unexposed) cultures ($p < 0.05$; Fig. 6). For the highest dose, the rate of cell proliferation was significantly greater than in control cultures through 8 days post-irradiation ($p < 0.05$; Fig. 6).

Laser irradiation of cell population using lower energy doses in the range of $0.1\text{--}1 \text{ J}/\text{cm}^2$ were also conducted

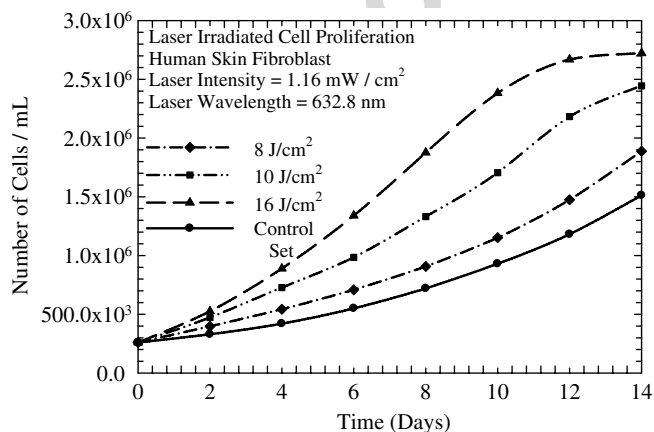


Fig. 5. Comparison of cell proliferation in control (un-irradiated) cultures and cultures in which the whole cell population was irradiated with various laser energy doses using a fan beam.

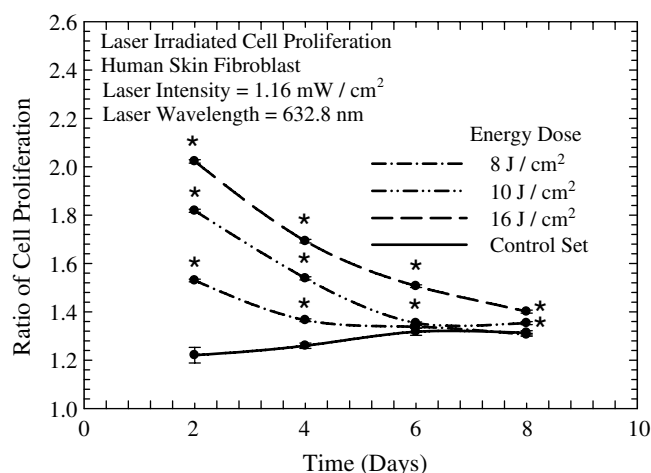


Fig. 6. Comparison of the rate of cell proliferation (ratio = number of cells on day indicated divided by number two days before) after irradiation of the whole cell population on day 0 with various laser energy doses using fan beam (control = un-irradiated cultures). * Mean values significantly different from control on that day (Welch's t -test, $p < 0.05$); error bars smaller than symbol size are omitted.

keeping laser intensity constant at $1.16 \text{ mW}/\text{cm}^2$ and it was observed that energy doses in this range had no significant effect on cell proliferation rate (data not shown).

Fig. 7 compares the ratio of cell proliferation as a function of time for two different laser intensities ($1.16 \text{ mW}/\text{cm}^2$ and $0.64 \text{ mW}/\text{cm}^2$) to the sham exposed control. Laser intensity was varied by varying laser power while keeping the spot size the same. Exposure durations were adjusted accordingly in order to keep a constant dose of $10 \text{ J}/\text{cm}^2$. It was observed that with higher laser intensity ($1.16 \text{ mW}/\text{cm}^2$) the ratio of cell proliferation was greater compared to the $0.64 \text{ mW}/\text{cm}^2$ ($p < 0.05$ for days 2 and 4). Both levels of laser intensities produced cell proliferation rates significantly greater than the sham exposed cell rates at 2–4 days post-irradiation ($p < 0.05$; Fig. 7).

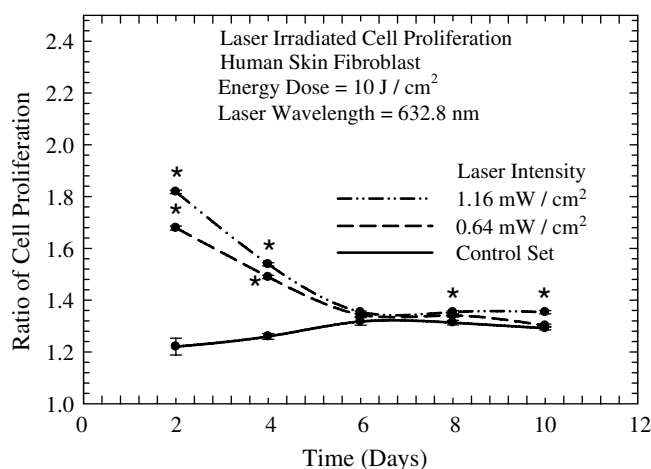


Fig. 7. Comparison of the ratio of cell proliferation for irradiation of the whole cell population with various laser intensities using fan beam. * Mean values significantly different from control on that day (Welch's t -test, $p < 0.05$); error bars smaller than symbol size are omitted.

3.3. Single cell irradiation using nano-probes and fluorescence life-time imaging of ROS

Fabricated fiber-optic nano-probes were used to deliver the laser light precisely onto a chosen adherent fibroblast cell. Precise manipulation of the nano-probe was accomplished through the use of a micromanipulator with micron-level precision of movement. Final location of the probe tip was determined using an inverted microscope to ensure that the nano-probe tip was touching a single cell. After the precise placement of the nano-probe, the 633 nm laser light was delivered on the cell.

Single cell experiments were conducted (a) by keeping a constant intensity of exposure and changing the time duration of exposure (i.e., the dose) and (b) by varying intensity by changing laser power and keeping the fluence dose constant. Under a single cell exposure treatment, only a few cells were seeded in a petri dish (which was achieved through serial dilutions). Very low adherent cell numbers seeded into the dish made it feasible for the irradiated cell to be tagged with a marker from the underside of the dish, thus enabling the irradiated tagged cell to be monitored under a high resolution phase contrast microscope several days post-laser radiation. It was observed under a phase contrast microscope for the case of varying laser doses that the irradiated cell and a few cells immediately surrounding the irradiated cell proliferated faster while the other cells which were further away from the irradiated cell did not show any enhancement in cellular proliferation rate. The bulk scale cell counting using the hemacytometer methodology yielded no measurable change in cell proliferation rate (data not shown). Evidently, the effect of single cell irradiation remained localized within a small confined region. On the other hand, no localized enhancement in cell growth was observed for the case of varying laser intensity unlike the case of varying laser dose and this lack of enhancement in cell growth is found to be consistent with the bulk cell irradiation findings.

According to pre-existing proposed models, ROS are important biochemical species within the cell which are believed to be responsible either for enhanced cell proliferation or cell destruction depending on their light induced intra-cellular levels. Monitoring biochemical processes is a first step which could help to explain the enhanced effect of cellular proliferation rate due to low power laser irradiation. Fluorescence life-time imaging of ROS were performed to investigate generation of ROS species.

The ROS chemical detection probe H₂DCFDA is light sensitive, and calibration of the background fluorescent intensity with fibroblast cells loaded with H₂DCFDA was performed without any LLLT (633 nm He–Ne) laser exposure on cells. The adherent fibroblast cells (within a Petri dish) were loaded with H₂DCFDA, and were excited with the probing 488 nm wavelength light (6 mW and 48 mW/cm²) from a Mercury lamp. The time-dependent decay of the background fluorescence (at 522 nm wavelength) was captured using a CCD camera at regular intervals of

0.2 s. This provided a temporal background fluorescence intensity profile which was due to the oxidization of H₂DCFDA by the excitation (488 nm wavelength) light source of the microscope. Life-time imaging of background fluorescent intensity are plotted in Fig. 8 for 2 days old cells and 4 days old cells in different Petri dishes. The temporal intensity profiles in both cases are identical, which implied that the background fluorescent intensity is independent of the age of individual cells and are equal magnitude under all experimental treatments considered herein.

After the temporal background fluorescent intensity was monitored, experiments were conducted on single cells loaded with H₂DCFDA by precisely delivering 8 and 20 J/cm² of He–Ne laser (633 nm wavelength) energy doses through nano-probes. The (He–Ne) laser intensity was kept constant while the time of irradiation was varied to achieve the desired energy dose on individual cells. Four different laser intensities – 125, 330, 1000, and 2000 mW/cm² were considered. Images of fluorescent intensity due to ROS generation were captured in an identical manner as it was done for baseline fluorescent intensity calibration. Fig. 9 exhibits a typical sample of images from a single cell at four different time points from the LLLT treatment condition of 8 J/cm² (exposure time of 24 s). The background fluorescence intensity was subtracted from each of the images. The corrected temporal fluorescence spectra for different energy doses and intensities are shown in Fig. 10.

The results of these tests show a complicated relationship among laser intensity, irradiation time, and emitted fluorescence intensity. With irradiation times ranging from 4 to 120 s, peak fluorescence intensity always occurred between 4 and 16 s. Thus, detectable ROS generation occurred prior to offset of the laser source, suggesting that either ROS generation peaks within 16 sec or that available fluorophore becomes saturated within 16 s. Higher intensities caused higher peak fluorescence signal and also caused peak fluorescence signal to occur later (Fig. 10, 330 vs. 165 mW/cm²). However, for a fixed intensity (330 and 165 mW/cm²) the variation of peak with the variation of

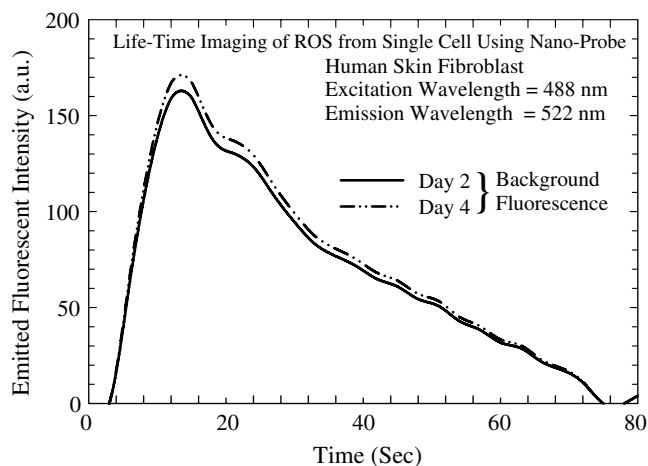


Fig. 8. Calibration of background fluorescence by ROS generated due to excitation source.

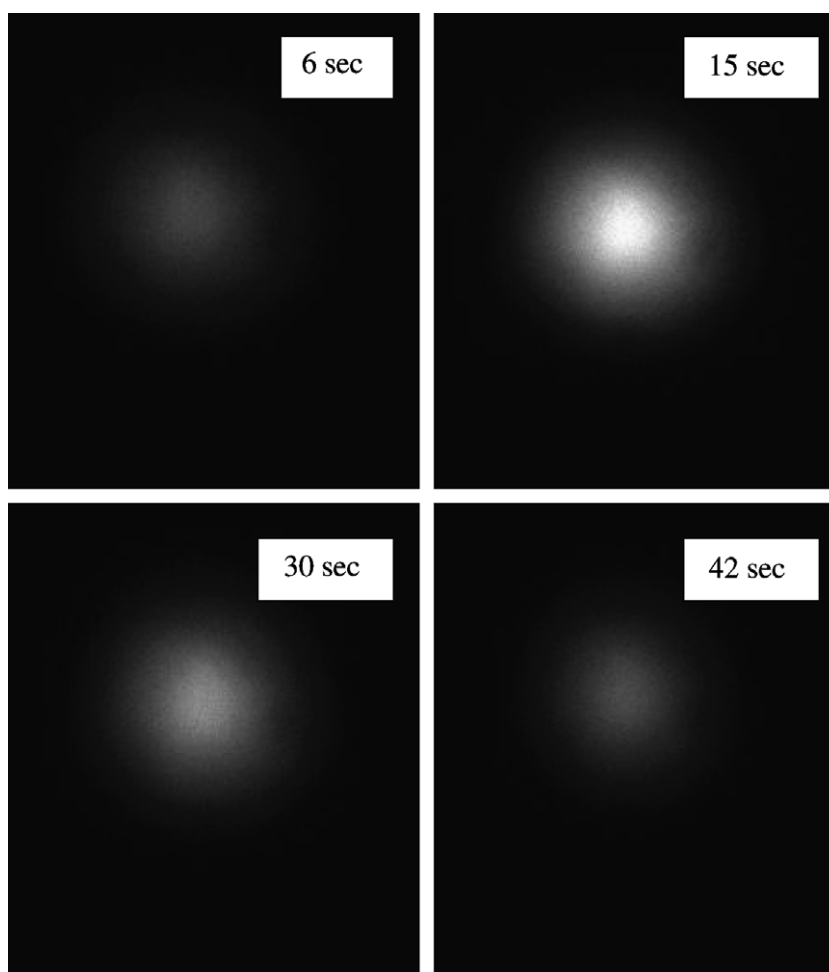


Fig. 9. Images of fluorescence emission due to ROS generation in response to laser irradiation of a single cell. Images were collected at the indicated times after the start of laser irradiation for 24 s for a total energy dose of 8 J/cm^2 .

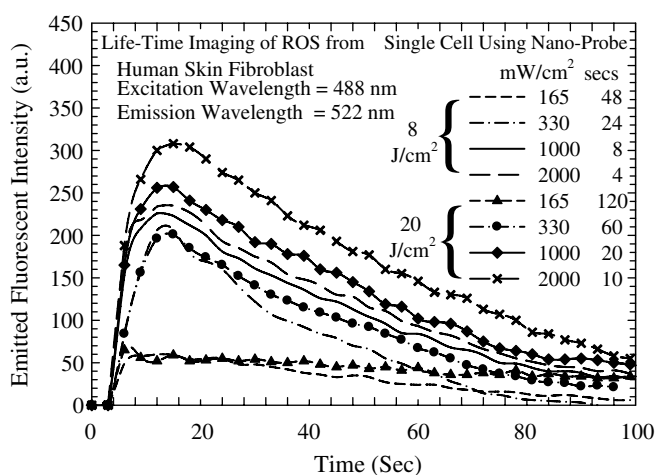


Fig. 10. Life-time imaging of corrected emitted fluorescence intensity due to ROS generation for the case of laser irradiation of a single cell using nano-probe with various laser intensities and energy doses. Variation in peak signal with the variation of energy dose is insignificant ($p > 0.05$, Welch's t -test) for laser intensities – 165 and 330 mW/cm^2 .

dose was found to be insignificant ($p > 0.05$). After the peak of fluorescence intensity, fluorescence levels gradually decreased, with longer laser irradiation times decreasing

the rate of fluorescence loss (Fig. 10, 165 mW/cm^2 , 120 vs. 48 s; 330 mW/cm^2 , 60 vs. 24 s).

The highest intensities tested were delivered with the shortest exposure times. In these cases, there was no discernable effect of irradiation time on the rate of decrease of the fluorescence signal (2000 mW/cm^2 , 10 vs. 4 s; 1000 mW/cm^2 , 20 vs. 8 s). There was, however, a very clear effect of time on the magnitude of the peak fluorescence signal; that is, longer exposure times produced higher peak fluorescence values (Fig. 10). Because in these cases the irradiation time was less than or near the time of peak fluorescence intensity, these individual cells received a greater total energy dose when irradiation times were longer. The initiation of H_2DCFDA fluorescence emission was found to be independent of the energy doses and intensities and started approximately 3 s after the He–Ne activation at $t = 0 \text{ s}$. Experiments for each case were repeated at least three times on different individual cells in different Petri dishes.

To observe the effect of simultaneous variation of energy doses and laser intensities keeping irradiation time constant in ROS generation, experiments were also performed on cells loaded with H_2DCFDA . The He–Ne laser energy was delivered to a single cell “instantaneously” (1 s

exposure) for each case. To achieve energy doses of 0.5, 1, 2, 4, 6, 8, and 20 J/cm² within 1 s, the laser intensity was varied from 500, 1000, 2000, 4000, 6000, 8000, and 20000 mW/cm², respectively. The corrected fluorescence spectra for different intensity of exposures are shown in Fig. 11. The value of peak intensity of emitted fluorescence is dependent on the total energy doses. In order to obtain the initial fluorescence signals for the case of 1 s exposure, the initial fluorescence spectra are shown in Fig. 11 inset. From Fig. 11 inset, it was observed that there was a delay in initiation of the emission of fluorescence for the case of 1 s exposures compared to the long time laser exposure as obtained from Fig. 10. This delay in the initiation of ROS generation increases with decreasing intensity and energy doses. The ROS generation for very high intensity and energy doses such as 20 J/cm² starts after 3 s, which is same as for the case of long time laser exposure of a single cell. The significant increase in peak fluorescence signal from 2 J/cm² to 4 J/cm² ($p < 0.05$) suggests the existence of threshold energy dose (4 J/cm²) below which the delay in the initiation of the emission of fluorescence is same for all energy doses, implying the ROS generation was very low to observe the differences.

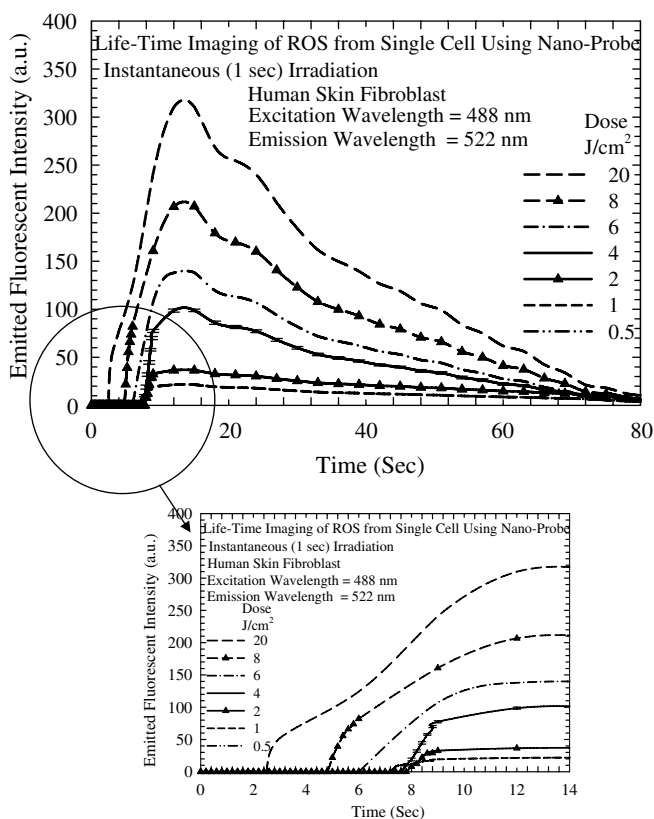


Fig. 11. Corrected fluorescence intensity kinetics due to ROS generation for the case of laser irradiation on a single cell using nano-probes with 1 s laser energy exposure. Significant increase in peak ($p < 0.05$, Welch's t -test) is observed for 4 J/cm² dose; standard errors of mean are calculated for all the experiments; however, the error bars are shown only for 4 J/cm² dose.

4. Conclusion

In this study the effects of low power laser irradiation on human skin fibroblast cells using nano-probes were investigated. It was demonstrated that there is an enhanced rate of cell proliferation after laser irradiation on entire cell population which was found to be primarily dependent on the laser energy dose. The effect of the laser stimulation lasted for a finite period of time under both schemes of exposure using various energy doses and laser intensities. Cellular proliferation rates were found to equal that of the controls six days post-laser treatment. By comparing the effect of laser irradiation on cell proliferation rate between parameters of total energy dose and laser intensity, respectively, it was deduced that laser intensity (over the intensity range of 0.64–1.16 mW/cm²) does not appear to have a strong dependency as compared to total energy dose parameter.

Nano-probes were demonstrated as a device to precisely deliver light on to a particular single cell. Irradiation of a single cell using nano-probes enabled real time transient ROS kinetics to be monitored during the low power light-cell interaction. The generation of ROS was observed to depend on both laser intensity and total laser energy dose delivered to a single cell using nano-probes. It is demonstrated that there exists a threshold energy dose for the case of instantaneous irradiation at which there is a change in the characteristics of ROS generation, such as the time-delay and the amount of ROS generation.

Single cell exposure with the aid of nano-probes enabled qualitative determination on the growth enhancement of the irradiated cell and its "sphere of influence" on the growth kinetics on neighboring cells.

This research can be furthered by monitoring effects of LLLT on individual cells in different phases in cell growth after LLLT to understand whether the effect of laser stimulation is beneficial or inhibitory to the cells at different growth phases in their cell cycle.

Acknowledgement

Kunal Mitra acknowledges support from National Science Foundation through grant BES 0406282. The authors would like to thank Dr. David J. Carroll, Associate Professor, Department of Biological Sciences, Florida Institute of Technology, FL, for assistance with experiments involving fluorescence life-time imaging.

References

- [1] T.I. Karu, Molecular mechanism of the therapeutic effect of low intensity laser irradiation, *Lasers Life Sci.* 2 (1988) 53–74.
- [2] H.H.F.L. van Breugel, P.R.D. Bar, Power density and exposure time of He–Ne laser irradiation are more important than total energy dose in photo-biomodulation of human fibroblasts in vitro, *Lasers Surg. Med.* 12 (1992) 528–537.
- [3] M. Boulton, J. Marshall, He–Ne laser stimulation of human fibroblast proliferation and attachment in vitro, *Lasers Life Sci.* 1 (1986) 125–134.

- [4] K.R. Byrnes, X. Wu, R.W. Waynant, I.K. Ilev, J.J. Anders, Low power laser irradiation alters gene expression of olfactory ensheathing cells in vitro, *Lasers Surg. Med.* 37 (2005) 161–171.
- [5] S.K. Snyder, K.R. Byrnes, R.C. Borke, A. Sanchez, J.J. Anders, Quantification of calcitonin gene-related peptide mRNA and neuronal cell death in facial motor nuclei following axotomy and 633 nm low power laser treatment, *Lasers Surg. Med.* 31 (2002) 216–222.
- [6] C. Broadley, K.N. Broadley, G. Disimone, L. Reinisch, J.M. Davidson, Low energy helium–neon laser irradiation and the tensile strength of incisional wounds in the rat, *Wound Rep. Reg.* 3 (1995) 512–517.
- [7] J.D.F. Allendorf, M. Bessler, J. Huang, M.L. Kayton, D. Laird, R. Nowygrod, M.R. Treat, Helium–neon laser irradiation at fluences of 1, 2, and 4 J/cm² failed to accelerate wound healing as assessed by both wound contracture rate and tensile strength, *Lasers Surg. Med.* 20 (1997) 340–345.
- [8] A.S. Lowe, M.D. Walker, M. O'Byrne, G.D. Baxter, D.G. Hirst, Effect of low intensity monochromatic light therapy (890 nm) on a radiation impaired, wound-healing model in murine skin, *Lasers Surg. Med.* 23 (1998) 291–298.
- [9] M.D. Walker, S. Rumpf, G.D. Baxter, D.G. Hirst, A.S. Lowe, Effect of low-intensity laser irradiation (660 nm) on a radiation-impaired wound-healing model in murine skin, *Lasers Surg. Med.* 26 (2000) 41–47.
- [10] R. Lubart, Y. Wollman, H. Friedman, S. Rochkind, I. Laulich, Effects of visible and near-infrared lasers on cell culture, *J. Photochem. Photobiol.* 12 (1992) 305–310.
- [11] P. Moore, T.D. Ridgway, R.G. Higbee, E.W. Howard, M.D. Lucroy, Effect of wavelength on low-intensity laser irradiation-stimulated cell proliferation in vitro, *Lasers Surg. Med.* 36 (2005) 8–12.
- [12] E. Alexandratou, D. Yova, P. Handris, D. Kletsas, S. Loukas, Human fibroblasts alterations induced by low power laser irradiation at the single cell level using confocal microscopy, *Photochem. Photobiol. Sci.* 1 (2002) 547–552.
- [13] N. Grossman, N. Schneid, H. Reuveni, S. Halevy, R. Lubart, 780 nm low power diode laser irradiation stimulates proliferation of keratinocyte cultures: Involvement of reactive oxygen species, *Lasers Surg. Med.* 22 (1998) 212–218.
- [14] R. Lubart, M. Eichler, R. Lavi, H. Friedman, A. Shainberg, Low-energy laser irradiation promotes cellular redox activity, *Photomed. Laser Surg.* 1 (2005) 3–9.
- [15] Y. Lin, A.H. Berg, P. Iyengar, T.K.T. Lam, A. Giacca, T.P. Combs, M.W. Rajala, X. Du, B. Rollman, W. Li, M. Hawkins, N. Barzilai, C.J. Rhodes, I.G. Fantus, M. Brownlee, P.E. Scherer, The hyperglycemia-induced inflammatory response in adipocytes: The role of reactive oxygen species, *J. Biol. Chem.* 280 (2005) 4617–4626.
- [16] R. Lubart, H. Friedman, T. Levinshal, R. Lavie, H. Breitbart, Effect of light on calcium transport in bull sperm cells, *J. Photochem. Photobiol. B: Biol.* 15 (1992) 337–341.
- [17] M. Tong, Y.F. Liu, X.N. Zhao, C.Z. Yan, Z.R. Hu, Z.H. Zhang, Effects of different wavelengths of low level laser irradiation on murine immunological activity and intracellular Ca²⁺ in human lymphocytes and cultured cortical neurogliaocytes, *Lasers Med. Sci.* 15 (2000) 201–206.
- [18] S.A. Gordon, K. Surrey, Red and far-red action on oxidative phosphorylation, *Radiat. Res.* 12 (1960) 325–339.
- [19] S. Passarella, E. Casamassima, S. Molinari, D. Pastore, E. Quagliariello, I.M. Catalano, A. Cingolani, Increase of proton electrochemical potential and ATP synthesis in rat liver mitochondria irradiated in vitro by helium–neon laser, *FEBS Lett.* 175 (1984) 95–99.
- [20] M. Schaffer, R. Sroka, C. Fuchs, U. Schrader-Reichardt, P.M. Schaffer, M. Busch, E. Duhmke, Biomodulative effects induced by 805 nm laser light irradiation of normal and tumor cells, *J. Photochem. Photobiol. B: Biol.* 40 (1997) 253–257.
- [21] J.M. Ocana-Quero, J.P. de la Lastra, R. Gomez-Villamandos, M. Moreno-Millan, Biological effect of helium–neon (He–Ne) laser irradiation on mouse myeloma (Sp2-Ag14) cell line in vitro, *Lasers Med. Sci.* 13 (1998) 214–218.
- [22] R. Hilf, R.S. Murant, U. Narayanan, S.L. Gibson, Relationship of mitochondrial function and cellular adenosine triphosphate levels to hematoporphyrin derivative induced photosensitization in R3230AC mammary tumors, *Cancer Res.* 46 (1986) 211–217.
- [23] V. Manteifel, L. Bakccva, T. Karu, Ultrastructure changes chondriome of human lymphocytes after irradiation of He–Ne laser: appearance of giant mitochondria, *J. Photochem. Photobiol. B: Biol.* 38 (1997) 25–30.
- [24] T.I. Karu, Photobiological fundamentals of low-power laser therapy, *IEEE J. Quantum Electron.* QE-23 (1987) 1703–1717.
- [25] H. Friedman, R. Lubart, I. Laulich, A possible explanation of laser-induced stimulation and damage of cell cultures, *J. Photochem. Photobiol. B: Biol.* 11 (1991) 87–95.
- [26] J.P. Singh, D.F. Babcock, H.A. Lardy, Motility activation, respiratory activation and alteration of Ca²⁺ transport in bovine sperm treated with amine local anesthetics and calcium transport antagonists, *Arch. Biochem. Biophys.* 221 (1983) 291–303.
- [27] H. Breitbart, R. Wehbie, H. Lardy, Calcium transport in bovine sperm mitochondria: effect of substrates and phosphate, *Biochim. Biophys. Acta* 1027 (1990) 72–78.
- [28] T.M. Buttke, P.A. Sandstorm, Oxidative stress as a mediator of apoptosis, *Immunol. Today* 15 (1994) 7–10.
- [29] N.H. Hunt, D.M. van Reyk, J.C. Fragonas, T.M. Jeitner, S.D. Goldstone, Redox mechanisms in T cell activation, in: C. Pasquier (Ed.), *Oxidative Stress, Activation, and Viral Infection*, Birkhauser Verlag, Basel, Switzerland, 1994, pp. 237–251.
- [30] L. Fialkow, C.K. Chan, S. Grinstein, G.P. Downey, Regulation of tyrosine phosphorylation in neutrophils by the NaDPH oxidase, *J. Biol. Chem.* 268 (1993) 17131–17137.
- [31] E. de Lamirande, H. Jiang, A. Zini, H. Kodama, C. Gagnon, Reactive oxygen species and sperm physiology, *Rev. Reprod.* 2 (1997) 48–54.
- [32] G.A. Callaghan, C. Riordan, W.S. Gilmore, I.A. McIntyre, J.M. Allen, B.M. Hannigan, Reactive oxygen species inducible by low-intensity laser irradiation alter DNA synthesis in the haemopoietic cell line U937, *Lasers Surg. Med.* 19 (1996) 201–206.
- [33] S.M. Barnard, D.R. Walt, A fiber optic chemical sensor with discrete sensing sites, *Nature* 353 (1991) 338–340.
- [34] O.S. Wolfbeis, *Fiber Optic Chemical Sensors and Biosensors*, CRC Press, Boca Raton, FL, 1991.
- [35] J.S. Schultz, *Biosensors*, *Sci. Am.* 265 (1991) 64–69.
- [36] B.M. Cullum, G.D. Griffin, G.H. Miller, T. Vo-Dinh, Intracellular measurements in mammary carcinoma cells using fiber-optic nanosensors, *Anal. Biochem.* 277 (2000) 25–32.
- [37] S. Barker, R. Kopelman, T. Meyer, M. Cusanovich, Fiber-optic nitric oxide-selective biosensors and nanosensors, *Anal. Chem.* 70 (1998) 971–976.
- [38] S. Barker, R. Kopelman, Development and cellular applications of fiber optic nitric oxide sensors based on a gold-adsorbed fluorophores, *Anal. Chem.* 70 (1998) 4902–4906.
- [39] I. Ilev, R. Waynant, All-fiber-optic sensor for liquid level measurement, *Rev. Sci. Instrum.* 70 (1999) 2551–2555.
- [40] E. Betzig, R.J. Chichester, Single molecules observed by near-field scanning optical microscopy, *Science* 262 (1993) 1422–1425.
- [41] E. Alexandratou, D. Yova, V. Atlamazoglou, P. Handris, D. Kletsas, S. Loukas, Low-power laser effects at single cell level: a confocal microscopy study, *Proc. SPIE* 4159 (2000) 25–33.
- [42] P.M. Powell, Low-power single-cell laser irradiation alters human fibroblasts, *Biophot. Int.* 9 (2002) 29–30.
- [43] D. Lapotko, T. Ramanovskaya, E. Gordiyko, Photothermal monitoring of respiratory chain redox state in single live cells, *Proc. SPIE* 4623 (2002) 314–323.